THE JOURNAL OF PHYSICAL CHEMISTRY C

Article

pubs.acs.org/JPCC

Functionalized Graphitic Carbon Nitride for Efficient Energy Storage

Menghao Wu,*[,†] Qian Wang,[†,‡] Qiang Sun,[†,‡] and Puru Jena[†]

[†]Department of Physics, Virginia Commonwealth University, Richmond, Virginia, 23284, United States

[‡]Center of Applied Physics and Technology, Peking University, Beijing 100871, China

ABSTRACT: Using first-principles calculations based on density functional theory, we show that recently synthesized graphitic carbon nitride (g-C_4N_3 and g-C_3N_4) can be functionalized with Li atoms for use as materials not only for high-capacity hydrogen storage but also for lithium-ion batteries. The unique properties are due to the high density of Li ions firmly adsorbed over nitrogen triangular holes. The gravimetric and volumetric densities of hydrogen in $Li_2C_3N_4$ and $Li_2C_4N_3$ are greater than 10 wt % and 100 g/L, respectively, both exceeding the target set by the U.S. Department of Energy. Similarly, single-layer $Li_2C_3N_4$ is a good candidate for a lithium-ion anode material with a specific capacity almost twice that of graphite, and bulk LiC_4N_3 can be used as a cathode material with a specific energy twice that of $LiCoO_2$. The materials have the added advantage that they are stable against clustering of Li and are nontoxic.

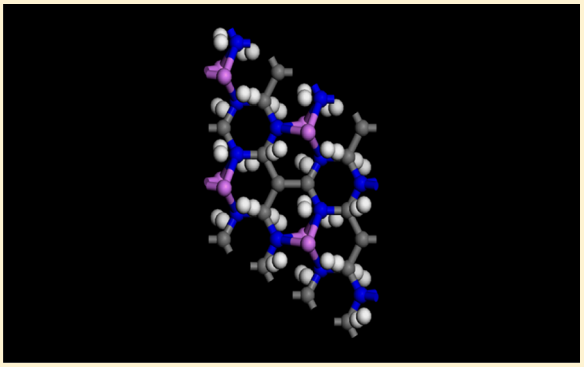

With dwindling supplies of fossil fuels and their adverse effects on the environment, there is currently considerable emphasis on developing clean renewable energies and finding materials for their efficient storage. In the transportation sector of the economy, hydrogen and batteries are among the important solutions.[1,2] Hydrogen storage materials for onboard applications have stringent requirements: They should be able to store hydrogen reversibly with large gravimetric and volumetric densities and operate at near-ambient thermodynamic conditions.[2−5] To date, no materials meet these industry requirements. Lithium-ion batteries are currently used as high-energy-density storage materials, but they suffer from high costs, safety concerns, and poor specific capacities. In addition, their cathode materials contain transition-metal atoms that are toxic and pose environmental risks.

In this article, we show that the graphitic carbon nitride materials g-C_3N_4[6] and g-C_4N_3,[7,8] which were recently synthesized by using cross-linking nitride-containing anions in ionic liquid, when suitably doped with Li, can address these challenges. The calculated gravimetric and volumetric densities of hydrogen in $Li_2C_3N_4$ and $Li_2C_4N_3$ are higher than 10 wt % and 100 g/L, respectively, and exceed the target set by the U.S. Department of Energy (DOE). In Li-ion batteries, single-layer $Li_2C_3N_4$ can serve as an anode material with a specific capacity almost twice that of graphite and bulk LiC_4N_3 can serve as a cathode material with a specific energy twice that of $LiCoO_2$. Equally important, these lithium-decorated graphitic carbon nitride materials are nontoxic and do not pose any environmental risk.

The above results are based on density functional theory (DFT) calculations performed using the DMol3 package.[9,10] The generalized gradient approximation (GGA) in the Perdew−Burke−Ernzerhof (PBE) form together with an all-electron double numerical basis set with polarized function (DNP basis set) were employed for the spin-unrestricted DFT computations.[11] The real-space global cutoff radius was set to 5.1 Å. After geometry optimization, forces on all atoms were less than 0.0002 Ha/Å. The results were verified using the Vienna Ab initio Simulation Package (VASP 5.2)[13−15] code with the GGA/PBE and PBE-D2 functionals of Grimme[12] for the exchange and correlation potential. Charges on atoms were calculated using Hirshfeld charge analysis.

A. Hydrogen Storage. For a successful hydrogen economy, it is essential to be able to store hydrogen efficiently and in large quantities. According to the U.S. DOE, the gravimetric and volumetric densities of hydrogen should be larger than 5.5 wt % and 81 g/L, respectively, and the materials should be operable at near-ambient thermodynamic conditions. To meet the gravimetric density requirement, these materials should be lighter than aluminum. Unfortunately, for elements lighter than aluminum, hydrogen binds either strongly with covalent or ionic bonds or weakly through van der Waals interaction. Consequently, the hydrogen desorption temperature is high for the former and low for the latter. For ideal desorption, the adsorption energy of H_2 should be between 0.2 and 0.6 eV per molecule.[16] Two mechanisms have been proposed that can accomplish this goal. The mechanism due to Kubas involves the interaction between a transition-metal atom and a hydrogen molecule, where the latter donates electrons to the unfilled d orbitals of the transition-metal atom, which then back-donates the electrons to the antibonding orbital of the hydrogen molecule.[17−19] The other mechanism, proposed by

Received: December 5, 2012
Revised: February 17, 2013
Published: March 7, 2013

   dx.doi.org/10.1021/jp311972f | J. Phys. Chem. C 2013, 117, 6055−6059

Niu et al.,[20] makes use of the polarization mechanism where a metal cation can bind a large number of H_2 molecules because of the electric field it produces. In both cases, hydrogen binds to the metal atom in quasimolecular form, with binding energies intermediate between those of physisorption and chemisorption. However, to maintain the stability of materials, it is important that these metal atoms not cluster. One way of achieving this goal is to find metal atoms that either bind to the substrate more strongly than they do to each other or are an integral part of the material. Although several predicted metal-doped nanostructured materials can store hydrogen with high gravimetric densities,[21−32] synthesizing these materials in bulk quantities remains a challenge. Ideally, what is needed is to decorate a bulk material that already exists with metal ions and to ensure that these ions do not cluster during multiple hydrogen adsorption/desorption cycles.[26] We show in this article that lithium-doped graphitic carbon nitrides (g-C_4N_3 and g-C_3N_4)[6−8] are such materials. Their applications in hydrogen storage[34] and reversible lithium intercalation[33,35] have already been experimentally studied. The polymorph of C_3N_4 used here is based on triazine, which is not as stable as that based on heptazine.[6] However, triazine-based C_3N_4 has been synthesized.[33] The reason for our studying the triazine-based C_3N_4 for energy storage is discussed later.

The structures of single layers of g-C_3N_4 and g-C_4N_3 are shown in panels a and b, respectively, of Figure 1. To determine

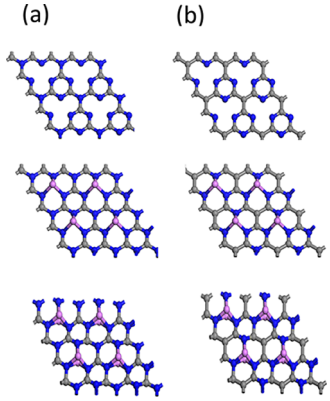

Figure 1. Geometric structures of (a) g-C_3N_4, g-LiC_3N_4, and g-$Li_2C_3N_4$, and (b) g-C_4N_3, g-LiC_4N_3, and g-$Li_2C_4N_3$. Gray, blue, and purple spheres denote carbon, nitrogen, and lithium atoms, respectively.

their preferred locations, Li atoms were placed over both the triangular N holes and the hexagonal rings, and the resulting structures were optimized. When the supercell of each g-C_3N_4 and g-C_4N_3 is decorated with one lithium atom, the lithium atom prefers to reside over the triangular N holes with binding energies of 2.2 and 4.3 eV per atom, respectively. The binding energies of Li atoms placed over the hexagonal rings of g-C_3N_4 and g-C_4N_3 are much smaller, namely, 0.35 and 2.1 eV, respectively. When two Li atoms are placed on the two sides in every supercell of g-C_3N_4 and g-C_4N_3, the Li atoms again prefer to reside over the triangular N holes with respective binding energies of 2.4 and 3.4 eV. The charges on the Li atoms in these two systems are 0.25e and 0.27e, respectively, and the average distances between the Li atoms and CN plane are 1.21 and 1.15 Å, respectively. This explains why the binding energy in $Li_2C_3N_4$ is smaller than that in $Li_2C_4N_3$. Because g-C_4N_3 can be thought of as N-doped g-C_3N_4, it is more inclined to accept one electron from every Li atom. Because these binding energies are all larger than the cohesive energy of bulk lithium, namely, 1.6 eV, lithium atoms do not cluster, and $Li_2C_3N_4$ and $Li_2C_4N_3$ are both stable. Vibrational calculations were performed on those systems, and no imaginary frequencies were found.

We next studied the interaction of hydrogen molecules with the Li atoms by first placing one H_2 molecule over a Li atom in every supercell of the $Li_2C_3N_4$ and $Li_2C_4N_3$ systems, as shown in the left panel of Figure 2. After optimization, the hydrogen

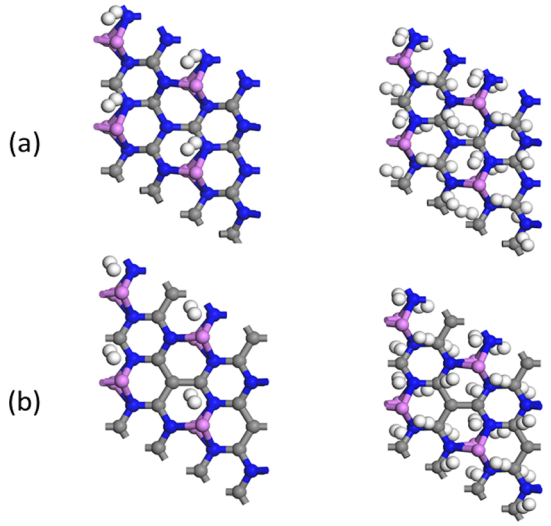

Figure 2. Geometric structures of (a) g-$Li_2C_3N_4$ and (b) g-$Li_2C_4N_3$ decorated with one and six hydrogen molecules in every supercell. Gray, white, blue, and purple spheres denote carbon, hydrogen, nitrogen, and lithium atoms, respectively.

atoms were all found to bind in quasimolecular form with a H−H distance of 0.76 Å. The distances between the hydrogen molecule and the Li atom in $Li_2C_3N_4$ and $Li_2C_4N_3$ systems were 2.50 and 2.18 Å, respectively. Up to three H_2 molecules could be adsorbed on every Li atom in these two systems (i.e., six hydrogen molecules in every supercell), as displayed in the right panel of Figure 2. The average distances between hydrogen molecules and the Li atoms were found to be 2.86 and 2.43 Å, respectively. We computed the adsorption energy of H_2 using different methods: (1) GGA/PBE implemented in DMol3, (2) LDA implemented in DMol3, (3) GGA/PBE implemented in VASP 5.2, and (4) the PBE-D2 method of Grimme implemented in VASP 5.2. As shown in Table 1, the adsorption energies calculated using the PBE functional in VASP and DMol3 are small but comparable. Because H_2 molecules are bound in quasimolecular form, it is important to include dispersive forces in the energy calculation. Because

Table 1. Calculated Adsorption Energy (eV) of Hydrogen Molecules Adsorbed on $Li_2C_3N_4$ and $Li_2C_4N_3$ Using Different Codes and DFT Functionals

	method			
host	PBE-DMol	LDA-DMol	PBE-VASP	PBE-D2-VASP
$Li_2C_3N_4$ ($1H_2$)	0.046	0.25	0.068	0.14
$Li_2C_3N_4$ ($6H_2$)	0.076	0.30	0.064	0.22
$Li_2C_4N_3$ ($1H_2$)	0.070	0.33	0.096	0.16
$Li_2C_4N_3$ ($6H_2$)	0.034	0.30	0.083	0.22

dx.doi.org/10.1021/jp311972f | J. Phys. Chem. C 2013, 117, 6055−6059

these are lacking at the DFT-PBE level of theory, we repeated the calculations using the PBE-D2 level of theory implemented in the VASP code. The resulting binding energies are a factor of 2 larger than those obtained using the PBE functional. We note that, because LDA overestimates binding, it can often compensate for the dispersive forces that are otherwise absent in DFT. The results, computed using LDA in DMol code, are included in Table 1. These values are larger than those computed at both the PBE and PBE-D2 levels. The actual adsorption energies are likely to be between the values obtained using the PBE-D2 and LDA methods. With every Li atom binding to three H_2 molecules, the hydrogen gravimetric densities of $Li_2C_3N_4$ and $Li_2C_4N_3$ are 10.2 and 10.3 wt %, respectively. In addition to exceeding the U.S. DOE target for gravimetric density, these materials also exceed the U.S. DOE target for volumetric density (>81 g/L). We determined the volumetric densities of $Li_2C_3N_4$ and $Li_2C_4N_3$ by stacking them layer by layer with interlayer distances set at 10 Å. The resulting volumetric density of hydrogen in both systems is 100.2 g/L, which is significantly greater than the U.S. DOE target of 81 g/L. The Li-decorated g-C_3N_4 and g-C_4N_3 materials have the advantages that the host substrates have already been synthesized in bulk quantities and the Li atoms anchored to the substrate have no tendency to cluster.

B. Lithium-Ion Battery. In a Li-ion battery, two electrodes (anode and cathode) are hosts of lithium and are separated by an electrolyte. Lithium atoms diffuse in or out of the electrodes during the charging and discharging processes. The open-circuit voltage (OCV), which is the equilibrium voltage difference between the two electrodes, depends on the lithium chemical potential difference between the anode and cathode. To achieve a high OCV, a large chemical potential difference is desirable. At present, the most widely used anode and cathode materials in lithium-ion batteries are layered LiC_6 and $LiCoO_2$.The high cost, toxicity, and chemical instability of the cathode materials at deep charge prevent their use for wider applications. In addition, only half of the theoretical capacity can be utilized.[36−38] Because Li-decorated carbon nitride materials contain a high density of lithium ions, they can be ideal candidates for lithium-ion battery cathode and anode materials. For example, a high reversible capacity of 1200 mA·h/g and stable cycling performance were recently obtained.[39] In another recent report, Sakaushi et al.[40] demonstrated that covalent triazine-based frameworks can be successfully used as anode and cathode materials for ambipolar supercapacitors with a high specific energy of 1084 W·h/kg.[40]

We found that $Li_2C_3N_4$ and $Li_2C_4N_3$ have specific capacities of 524 and 534 mA·h/g, respectively, which are almost twice that of LiC_6 (372 mA·h/g). Because the binding energy of Li atoms in $Li_2C_3N_4$ is 2.4 eV, it is suitable for an anode material. $Li_2C_3N_4$ and LiC_3N_4 can also be rolled into nanotubes (NTs), similarly to graphene in carbon nanotubes (CNTs), as shown in Figure 3a,b. Here, the binding energies of Li atoms are 2.8 and 2.0 eV for $Li_2C_3N_4$ and LiC_3N_4, respectively, and these nanotubes can be made into three-dimensional bundles and applied as anodes.

$Li_2C_3N_4$ is not suitable for an anode material because the binding energy of Li is large. However, if $Li_2C_3N_4$ were applied as a cathode material, the maximum specific energy could reach 0.961 kW·h/kg, which is almost twice that of $LiCoO_2$ (0.518 kW·h/kg). However, the OCV here is only 1.6 V, which is much smaller than that of $LiCoO_2$ (around 3.5 V). To enhance the OCV, we considered intercalating lithium ions into the

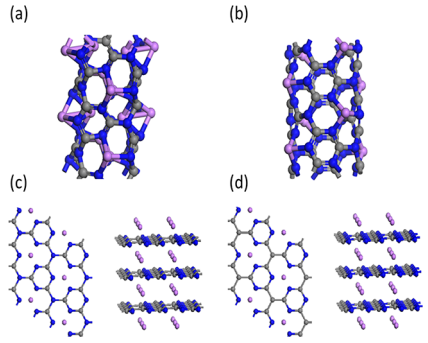

Figure 3. Geometric structures of (a) $Li_2C_3N_4$ (4,4) nanotube (NT), (b) LiC_3N_4 (4,4) NT, (c) bulk LiC_3N_4, and (d) bulk LiC_4N_3.

layers of g-C_3N_4 and g-C_4N_3, as shown in Figure 3c,d. In bulk LiC_3N_4 and LiC_4N_3, every lithium ion is placed between two holes of two adjoining layers, and the specific capacities are reduced by 50% compared to those of $Li_2C_3N_4$ and $Li_2C_4N_3$, as they contain half the number of lithium ions. However, the cohesive energies of lithium are 3.6 and 5.2 eV, respectively, so their OCVs are enhanced to 1.8 and 3.4 eV, respectively. As a result, when bulk LiC_4N_3 is used as a cathode material, the OCV can be doubled, and its maximum specific energy is even higher (0.974 kW·h/kg). This potential organic cathode material compared to that currently used in lithium-ion batteries is also environmentally friendly because it does not contain any toxic transition metals.

Because the heptazine-based units are more stable than the triazine-based ones for C_3N_4, it is likely that the former might be mixed with the latter when synthesized experimentally. Therefore, we investigate the potential of Li-doped heptazine-based C_3N_4 for energy storage. As shown in Figure 4a, for every

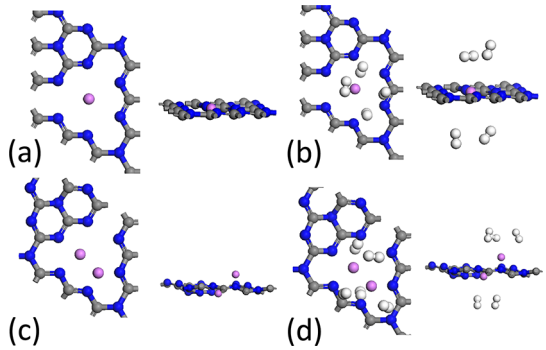

Figure 4. Geometric structures of (a) heptazine-based LiC_6N_8, (b) heptazine-based LiC_6N_8 with four hydrogen molecules per supercell, (c) heptazine-based $Li_2C_6N_8$, and (d) heptazine-based $Li_2C_6N_8$ with five hydrogen molecules per supercell.

C_6N_8 unit in a supercell, when one Li atom is adsorbed, the binding energy of the Li atom is 3.3 eV/atom, and the optimized system remains planar. The ability to adsorb hydrogen molecules is affected by the planar structure, as lithium atoms have more space to adsorb hydrogen molecules when they are out of the plane. As shown in Figure 4b, every heptazine-based LiC_6N_8 can adsorb four H_2 molecules, resulting in a hydrogen gravimetric density of 4.0 wt %. When two Li atoms are adsorbed in every C_6N_8 unit in a supercell, the average binding energy of Li atom is reduced to 3.1 eV/atom. As shown in Figure 4c, the optimized system becomes distorted, with one Li atom residing on the CN plane

dx.doi.org/10.1021/jp311972f | J. Phys. Chem. C 2013, 117, 6055−6059

and the other being out of the plane. In Figure 4d, every heptazine-based $Li_2C_6N_8$ can adsorb five H_2 molecules, two by the Li atom in the plane and three by the one out of the plane, resulting in a hydrogen gravimetric density of 4.8 wt %. This is much less than that adsorbed by triazine-based $Li_2C_3N_4$. For C_4N_3, the only polymorph that has been synthesized, to our knowledge, is triazine-based.[7] In a recent experimental study of the lithiation of g-C_3N_4,[41] it was reported that the addition of Li to heptazine-based C_3N_4 results in an irreversible reaction leading to the formation of Li—CH═NR and Li—N═CR_2 species. Carbon nitride suitable for the anode needs a high density of pyridinic C−N−C terminal bonds and a low density of quaternary C_3N species to boost the electronic conductivity and reversible cycling of Li ions. In comparison, C_4N_3 does not have such quaternary C_3N species. In addition, because C_4N_3 is essentially p-doped and is inclined to obtain one additional electron for every unit cell, LiC_4N_3 is even more stable than C_4N_3. Therefore, for applications in hydrogen storage and lithium batteries, C_4N_3 is more desirable than C_3N_4.

In summary, using total energy calculations, we demonstrated that lithium-decorated g-C_4N_3 and g-C_4N_3 are good candidates for high-capacity energy storage; they can be used as hydrogen storage materials and lithium-ion battery anode and cathode materials. These desirable properties are due to their high densities of nitrogen triangular holes where lithium ions are adsorbed. The adsorption energies of hydrogen molecules on Li atoms are ideally suited for efficient hydrogen sorption, and the predicted weight percentage of H_2 (>10 wt %) and volumetric density (>100 g/L) exceed the target values set by the U.S. Department of Energy. Single-layer $Li_2C_3N_4$ with a specific capacity almost twice that of graphite is a good candidate for a lithium-ion anode material, and bulk LiC_4N_3 with a specific energy twice that of $LiCoO_2$ can be used as a cathode material. These materials have the added advantages that they are nontoxic and pose no environmental risk. We hope that our predictions will stimulate experimental studies to explore the potential of these materials for efficient energy storage.

AUTHOR INFORMATION

Corresponding Author

*E-mail: mwu2@vcu.edu. Address: 701 W Grace St., Department of Physics, Virginia Commonwealth University, Richmond, VA, 23284.

Notes

The authors declare no competing financial interest.

ACKNOWLEDGMENTS

This work was supported in part by the U.S. Department of Energy. Resources of the National Energy Research Scientific Computing Center supported by the Office of Science of the U.S. Department of Energy under Contract DE-AC02-05CH11231 are also acknowledged.

REFERENCES

(1) Schlapbach, L.; Zuttel, A. Hydrogen-Storage Materials for Mobile Applications. *Nature* **2001**, *414*, 353−358.
(2) Liang, M.; Zhi, L. Graphene-Based Electrode Materials for Rechargeable Lithium Batteries. *J. Mater. Chem.* **2009**, *19*, 5871−5978.
(3) Crabtree, G. W.; Dresselhaus, M. S.; Buchanan, M. V. The Hydrogen Economy. *Phys. Today* **2004**, *57* (12), 39−44.
(4) Dinca, M.; Long, J. R. Hydrogen Storage in Microporous Metal−Organic Frameworks with Exposed Metal. *Angew. Chem., Int. Ed.* **2008**, *47*, 6766−6779.
(5) Jena, P. Materials for Hydrogen Storage: Past, Present, and Future. *J. Phys. Chem. Lett.* **2011**, *2*, 206−211.
(6) Kroke, E.; Schwarz, M.; Horath-Bordon, E.; Kroll, P.; Noll, B.; Norman, A. D. Tri-*s*-triazine Derivatives. Part I. From Trichloro-tris-*s*-triazine to Graphitic C_3N_4 Structures. *New J. Chem.* **2002**, *26*, 508−512.
(7) Lee, J. S.; Wang, X. Q.; Luo, H. M.; Dai, S. Fluidic Carbon Precursors for Formation of Functional Carbon under Ambient Pressure Based on Ionic Liquids. *Adv. Mater.* **2010**, *22*, 1004−1007.
(8) Du, A.; Sanvito, S.; Smith, S. C. First-Principles Prediction of Metal-Free Magnetism and Intrinsic Half-Metallicity in Graphitic Carbon Nitride. *Phys. Rev. Lett.* **2012**, *108*, 197207.
(9) Delley, B. Numerical Method for Solving the Local Density Functional for Polyatomic Molecules. *J. Chem. Phys.* **1990**, *92*, 508−517.
(10) Delley, B. From Molecules to Solids with the DMol3 Approach. *J. Chem. Phys.* **2000**, *113*, 7756−7764.
(11) Perdew, J. P.; Burke, K.; Ernzerhof, M. Generalized Gradient Approximation Made Simple. *Phys. Rev. Lett.* **1996**, *77*, 3865.
(12) Grimme, S. Semiempirical GGA-Type Density Functional Constructed with a Long-Range Dispersion Correction. *J. Comput. Chem. Soc.* **2006**, *27*, 1787−1799.
(13) Kresse, G.; Hafner, J. Ab Initio Molecular Dynamics for Liquid Metals. *Phys. Rev. B* **1993**, *47*, 558.
(14) Kresse, G.; Furthmuller, J. Efficient Iterative Schemes for ab initio Total-Energy Calculations Using a Plane-Wave Basis Set. *Phys. Rev. B* **1996**, *54*, 11169.
(15) Kresse, G.; Joubert, D. From Ultrasoft Pseudopotentials to the Projector Augmented-Wave Method. *Phys. Rev. B* **1999**, *59*, 1758.
(16) Kim, Y.; Zhao, Y.; Williamson, A.; Heben, M. J.; Zhang, S. B. Nondissociative Adsorption of H_2 Molecules in Light-Element-Doped Fullerenes. *Phys. Rev. Lett.* **2006**, *96*, 016102.
(17) Kubas, G. J. Metal−Dihydrogen and σ-Bond Coordination: The Consummate Extension of the Dewar−Chatt−Duncanson Model for Metal−Olefin π Bonding. *J. Organomet. Chem.* **2001**, *635*, 37−68.
(18) Philips, A. B.; Shivaram, B. S. High Capacity Hydrogen Absorption in Transition Metal−Ethylene Complexes Observed via Nanogravimetry. *Phys. Rev. Lett.* **2008**, *100*, 105505.
(19) Hu, X.; Skadtchenko, B. O.; Trudeau, M.; Antonelli, D. M. Hydrogen Storage in Chemically Reducible Mesoporous and Microporous Ti Oxides. *J. Am. Chem. Soc.* **2006**, *128*, 11740−11741.
(20) Niu, J.; Rao, B. K.; Jena, P. Binding of Hydrogen Molecules by a Transition Metal Ion. *Phys. Rev. Lett.* **1992**, *68*, 2277.
(21) Park, N.; Hong, S.; Kim, G.; Jhi, S.-H. Computational Study of Hydrogen Storage Characteristics of Covalent-Bonded Graphenes. *J. Am. Chem. Soc.* **2007**, *129*, 8999−9003.
(22) Zhao, Y.; Kim, Y.-H.; Dillon, A. C.; Heben, M. J.; Zhang, S. B. Hydrogen Storage in Novel Organometallic Buckyballs. *Phys. Rev. Lett.* **2005**, *94*, 155504.
(23) Yildirim, T.; Ciraci, S. Titanium-Decorated Carbon Nanotubes as a Potential High-Capacity Hydrogen Storage Medium. *Phys. Rev. Lett.* **2005**, *94*, 175501.
(24) Meng, S.; Kaxiras, E.; Zhang, Z. Metal−Diboride Nanotubes as High-Capacity Hydrogen Storage Media. *Nano Lett.* **2007**, *7*, 663−667.
(25) Sun, Q.; Wang, Q.; Jena, P.; Kawazoe, Y. Clustering of Ti on a C_{60} Surface and Its Effect on Hydrogen Storage. *J. Am. Chem. Soc.* **2005**, *127*, 14582−14583.
(26) Wu, M.; Gao, Y.; Zhang, Z.; Zeng, X. C. Edge-Decorated Graphene Nanoribbons by Scandium as Hydrogen Storage Media. *Nanoscale* **2012**, *4*, 915−920.
(27) Yoon, M.; Yang, S.; Wang, E.; Zhang, Z. Fullerenes as High-Capacity Hydrogen Storage Media. *Nano Lett.* **2007**, *7*, 2578−2583.
(28) Deng, W.-Q.; Xu, X.; Goddard, W. A. New Alkali Doped Pillared Carbon Materials Designed to Achieve Practical Reversible

Hydrogen Storage for Transportation. *Phys. Rev. Lett.* **2004**, *92*, 166103.
(29) Sun, Q.; Jena, P.; Wang, Q.; Marquez, M. First-Principles Study of Hydrogen Storage on $Li_{12}C_{60}$. *J. Am. Chem. Soc.* **2006**, *128*, 9741−9745.
(30) Lee, H.; Ihm, J.; Cohen, M. L.; Louie, S. G. Calcium-Decorated Graphene-Based Nanostructures for Hydrogen Storage. *Nano Lett.* **2010**, *10*, 793−798.
(31) Dimitrakakis, G. K.; Tylianakis, E.; Froudakis, G. E. Pillared Graphene: A New 3-D Network Nanostructure for Enhanced Hydrogen Storage. *Nano Lett.* **2008**, *8*, 3166−3170.
(32) Du, A.; Zhu, Z.; Smith, S. C. Multifunctional Porous Graphene for Nanoelectronics and Hydrogen Storage: New Properties Revealed by First Principle Calculations. *J. Am. Chem. Soc.* **2010**, *132*, 2876−2877.
(33) Yang, X.; Wang, H.; Lu, X.; Cui, D.; Zhang, Z. Solid-State Synthesis of Graphite-like C_3N_4 and Its Reversible Li Intercalation. *Acta Chim. Sin.* **2009**, *67*, 1166−1170.
(34) Bai, X. D.; Zhong, D.; Zhang, G. Y.; Ma, X. C.; Liu, S.; Wang, E. G.; Chen, Y.; Shaw, D. T. Hydrogen Storage in Carbon Nitride Nanobells. *Appl. Phys. Lett.* **2001**, *10*, 1552−1554.
(35) Zhong, D. Y.; Zhang, G. Y.; Liu, S.; Wang, E. G.; Wang, Q.; Li, H.; Huang, X. J. Lithium Storage in Polymerized Carbon Nitride Nanobells. *Appl. Phys. Lett.* **2001**, *10*, 3500−3502.
(36) Manthiram, A. Materials Challenges and Opportunities of Lithium Ion Batteries. *J. Phys. Chem. Lett.* **2011**, *2* (3), 176−184.
(37) Armand, M.; Tarascon, J.-M. Building Better Batteries. *Science* **2008**, *451*, 652−657.
(38) Kang, B.; Ceder, G. Battery Materials for Ultrafast Charging and Discharging. *Nature* **2009**, *458*, 190−193.
(39) Mao, Y.; Duan, H.; Xu, B.; Zhang, L.; Hu, Y.; Zhao, C.; Wang, Z.; Chen, L.; Yang, Y. Lithium Storage in Nitrogen-Rich Mesoporous Carbon Materials. *Energy Environ. Sci.* **2012**, *5*, 7950−7955.
(40) Sakaushi, K.; Nickerl, G.; Wisser, M. F.; Nishio-Hamane, D.; Hosono, E.; Zhou, H.; Kaskel, S.; Eckert, J. An Energy Storage Principle Using Bipolar Porous Polymeric Frameworks. *Angew. Chem., Int. Ed.* **2012**, *27*, 7850−7854.
(41) Veith, G.; Baggeto, L.; Adamczyk, L. A.; Guo, B.; Brown, S. S.; Sun, X.; Albert, A. A.; Humble, J. R.; Barnes, C. E.; Bojdys, M. J.; Dai, S.; Dudney, N. J. Electrochemical and Solid-State Lithiation of Graphitic C_3N_4. *Chem. Mater.* **2013**, *25* (3), 503−508.